Analysis of Blockage Sensing by Radars in Random Cellular Networks

Jeonghun Park and Robert W. Heath Jr.

Abstract—**We characterize the detection probability of blockage sensing by radars deployed on towers in cellular networks. If the signal-to-interference ratio of the reflected pilot signal is larger than the predefined threshold and there is no other blockage between the radar and the corresponding blockage, the radar successfully detects the blockage. Modeling radar and blockage locations using stochastic geometry, we derive the detection probability as a function of the system parameters, chiefly the radar and blockage densities. Leveraging the obtained expression, we provide some guidelines for efficiently deploying radars to enhance the detection probability.**

Index Terms—**Radars, stochastic geometry, cellular networks, blockage sensing.**

I. Introduction

In emerging applications supported by wireless communications technologies, blockage detection is useful. For example, knowledge of blockages is side information for reconfiguring mmWave communications beams [1], [2]. The blockages themselves also provide situational awareness for automated driving. For sensing blockages in the entire street, base station towers can be used and the blockage information is delivered to vehicles by using vehicle-to-infrastructure communications [3]. Conventional approaches for blockage detection involve an initialization phase that may include beam training [4] or compressive channel estimation [5], which becomes a source of overhead when there is significant mobility. An alternative approach to manage blockage events is to use radars [1] to help detect blockages that can be detected or avoided. This motivates codeploying radars with the communications infrastructure. In this letter, we analyze the detection performance using radars with a random network model. Based on the analysis, we show how the detection performance changes depending on the radar deployment density, blockage density, or radar sensing beamwidth.

There is some prior work on spectrum sharing between radar and cellular communications. In [6], a cellular network shares spectrum with rotating radars. The base stations reduce their transmit power when the radar's main beam points to them, so that the harmful effect of communications interference at the radar decreases. In [7], an MIMO communications system and an MIMO radar operate on the same spectrum. Beamforming methods were designed to mitigate the interference caused by the MIMO communications system on the MIMO radar. The prior work [6], [7] considers couse of communications and radar in the same spectrum, whereas we suppose that the radar is operating in its own dedicated spectrum. Further, the analysis of detection probability in that prior work assumed a few neighboring radars whose locations are deterministic. This works for small networks, but does not extend to large and dense cellular networks.

Stochastic geometry is a useful tool for analyzing large networks by providing a means to calculate the interference distributions. Prior work derived the probability of detecting other vehicles considering an automotive application where the vehicles are equipped with radar [8]. The network topology though was linear, making it difficult to extend the results to two-dimensional (2-D) deployments and blockages.

In this letter, we analyze the blockage detection probability in a cellular radar deployment. We assume that radars and blockages are distributed in a 2-D space according to homogeneous Poisson point processes (PPPs). We consider a noncooperative individual blockage sensing scenario, where a single radar detects one blockage, modeled as a line segment, without cooperating with other radars. Assuming that the typical blockage is located at the origin, the radar closest to the origin is responsible for detecting the typical blockage. For successful detection, we assume the following two conditions. 1) The signal-to-interference ratio (SIR) of the reflected pilot signal should be larger than a specific threshold. 2) There is no other blockage except for the typical blockage in the sensing region of the corresponding radar. Under these assumptions, we derive the detection probability as system parameters such as radar and blockage densities, the size of the typical blockage, and the sensing beamwidth. Leveraging the derived expressions, we illustrate how the detection probability changes depending on the system parameters such as the radar density, the blockage density, or the beamwidth used in radar sensing. These results provide guidelines to improve the blockage detection performance. For example, deploying more radars in a cellular network is beneficial to blockage detection performance, but only if they use the appropriate beamwidth.

II. System Model

In this section, we describe the system model assumed in this paper. First we explain how radars and blockages are spatially

Manuscript received June 1, 2018; revised July 27, 2018; accepted August 26, 2018. Date of publication September 19, 2018; date of current version September 20, 2018. This work was supported in part by the National Science Foundation under Grant 1711702 and Grant 1731658, and in part by a gift from the Nokia Foundation. The associate editor coordinating the review of this manuscript and approving it for publication was Dr. Pu Wang. *(Corresponding author: Robert W. Heath.)*

J. Park is with the Qualcomm Wireless R&D, San Diego, CA 92121 USA (e-mail: jeonghun@utexas.edu).

R. W. Heath Jr. is with the Wireless Networking and Communication Group, Department of Electrical and Computer Engineering, The University of Texas at Austin, Austin, TX 78701 USA (e-mail: rheath@utexas.edu).

Color versions of one or more of the figures in this letter are available online at http://ieeexplore.ieee.org.

Digital Object Identifier 10.1109/LSP.2018.2869279

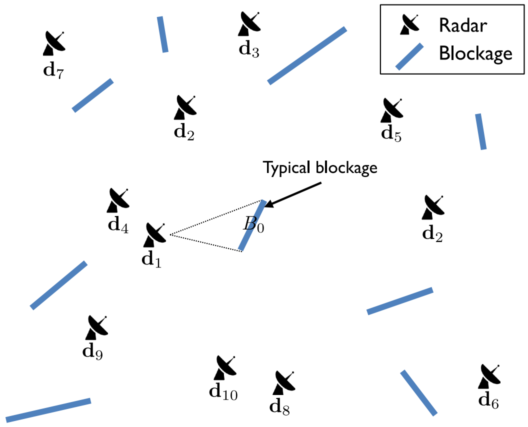

Fig. 1. Typical blockage B_0 is located at the origin. The tagged radar located $\mathbf{d}_1$ is responsible for detecting the typical blockage. In the detection process, the reflected signal is used.

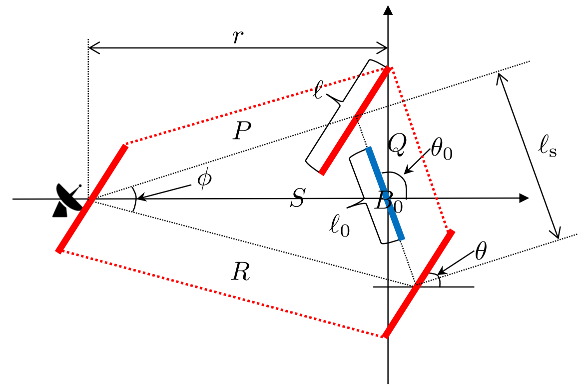

Fig. 2. Illustration of the typical blockage B_0 and other possible blockages. If there is no other blockage in the pentagon $T = P + Q + R + S$, the second condition for successfully detecting the typical blockage is satisfied. Additionally, we also get some intuition regarding the cross-section area A_σ in this figure. If the blockage length ℓ_0 is smaller than the sensing length ℓ_s, i.e., $\ell_0 < \ell_s$ as shown in the figure, the cross-section area is $A_\sigma = \ell_0 \sin(\theta_0)$. If $\ell_0 > \ell_s$, then we have $A_\sigma = \ell_s \sin(\theta_0)$.

distributed. Subsequently, we define the successful detection probability.

A. Radar and Blockage Location Model

We consider a cellular network that consists of randomly located radars and blockages. We model the radar locations as an independent homogeneous PPP denoted as $\Phi_{\mathrm{R}} = \{\mathbf{d}_i \in \mathbb{R}^2, i \in \mathbb{N}\}$ with density λ_{R}. We use a line Boolean model as in [9] to model the blockages. Lines are simple abstractions for more complicated shapes that permit tractable analysis. The center of the line is distributed as an independent homogeneous PPP with density λ_{B}. The length and the orientation of each blockage is uniformly distributed, written as $\ell_i \sim \mathcal{U}(0, L)$ and $\theta_i \sim \mathcal{U}(0, \pi)$, respectively, for $i \in \mathbb{N}$. We assume that the typical blockage, denoted as B_0, is located at the origin. As per Slivnyak's theorem, the detection performance of the typical blockage represents that of the whole networks. We also assume that the length and the orientation of the typical blockage are ℓ_0 and θ_0, respectively, without loss of generality.

We consider a noncooperative individual sensing scenario. Networked radars could perform joint detection, which can improve the blockage detection performance. This is interesting future work. Focusing on the typical blockage, the radar closest to the origin is responsible to detect the typical blockage. A snapshot of the considered blockage sensing scenario is illustrated in Fig. 1. As shown in Fig. 1, the radar located at $\mathbf{d}_1$ detects the typical blockage since $\|\mathbf{d}_1\| < \|\mathbf{d}_i\|$ for $i \geq 2$. We refer to the radar located at $\mathbf{d}_1$ as the tagged radar. Without loss of generality, we assume that the tagged radar is horizontally located with the center of the typical blockage as drawn in Fig 2.

B. Radar Signal-to-Interference-Plus-Noise Ratio (SINR) Model

We first explain the blockage detection process used in each radar. Considering a given time slot, a radar broadcasts a pilot sequence to a particular direction. To do this, we assume that each radar uses directional beamforming with main-lobe beamwidth ϕ. After that, a radar measures the reflected signal's power received within the main-lobe direction. We assume that each radar randomly selects a pilot sequence to use, so that a radar can obtain benefits of interference reduction from cross-correlation gain if interfering radars use different pilot sequence. Based on the received signal power, a radar determines whether a blockage exists in the current direction. In the next time slot, the radar changes the direction and repeats this process. Now we describe the effective SINR of the blockage detection process. Focusing on a particular time slot and the tagged radar, the SINR of the reflected pilot sequence is

$$\mathrm{SINR} = \frac{G_s P_t G^2 \left(\frac{c}{4\pi f}\right)^2 \frac{A_\sigma}{4\pi} r^{-4} |h_1|^2}{P_t G^2 \left(\frac{c}{4\pi f}\right)^2 \sum_{i=2}^{\infty} G_i \left\|\mathbf{d}_i - \mathbf{d}_1\right\|^{-\beta} |h_i|^2 + N_0} \tag{1}$$

where G_s is the auto-correlation gain and g_s is the cross-correlation gain of a pilot sequence. If a radar located at $\mathbf{d}_i$ uses the same pilot sequence with the tagged radar, $G_i = G_s$, otherwise $G_i = g_s$. Since each radar randomly selects a pilot sequence, the probability of $G_i = G_s$ is $1/N$ $\forall i$, where N is the number of sequences used in a whole network. Next, G is the antenna gain (the same transmit/receive antenna gains are assumed), c is the speed of light, and f is the operating frequency, A_σ is the cross-section area of the typical blockage, r is the distance between the tagged radar and the typical blockage, $|h_i|^2 \sim \mathrm{Exp}(1)$ is the fading coefficient from the radar location $\mathbf{d}_i$ to $\mathbf{d}_1$ (Rayleigh fading is assumed), N_0 is the noise variance, and β is the path-loss exponent. In addition, we assume that the interference links are in the same single state for analytical simplicity. Incorporating multiple link states is future work.

C. Performance Metric

In this letter, we assume two conditions for successful detection. First, the SINR (1) should be larger than the predetermined threshold γ. Note that this is a typical condition for detection problems used in other prior work [8] too. The probability of this first condition is $\mathbb{P}\left[\mathrm{SINR} > \gamma\right]$. Second, there should be no other blockage in the sensing region of the tagged radar except for the typical blockage. If the typical blockage is blocked by any other blockage, the tagged radar cannot detect the typical blockage perfectly. We denote the event that the typical blockage is blocked by other blockage as E_{block}.

Considering both conditions, the successful detection probability is

$$\begin{aligned}P_{\mathrm{detect}}(\gamma) &= \mathbb{P}\left[\{\mathrm{SINR} > \gamma\} \cap \{E_{\mathrm{block}}\}^c\right]\\ &\overset{(a)}{=} \mathbb{E}_r\left[\mathbb{P}\left[\mathrm{SINR} > \gamma | r\right] \cdot \mathbb{P}\left[\{E_{\mathrm{block}}\}^{\mathrm{c}} | r\right]\right]\end{aligned} \tag{2}$$

where (a) follows the assumption that every blockage is distributed independently, given the distance to the typical blockage r.

III. Performance Characterization

In this section, we analyze the detection probability (2). We consider the interference-limited regime in this letter. Note that typical radar scenarios are rarely interference limited. A difference in our scenario is that radars are densely deployed in a cellular network, so that the path loss to the typical blockage is relatively small compared to that of other scenarios. This justifies the interference-limited assumption. Under this assumption, noise is neglected and thus the term $P_t(Gc/(4\pi f))^2$ cancels out.

A. SIR Distribution

We first obtain the conditional SIR distribution $\mathbb{P}\left[\mathrm{SIR} > \gamma | r\right]$. Lemma 1 is the main result of this section.

Lemma 1: The SIR distribution conditioned on r and A_σ is

$$\begin{aligned}&\mathbb{P}\left[\mathrm{SIR} > \gamma | r, A_\sigma\right]\\ &= e^{\left(-\frac{\lambda_{\mathrm{R}}}{N}\frac{\pi\left(\frac{4\pi}{A_\sigma}r^4\gamma\right)^{2/\beta}}{\mathrm{sinc}\left(\frac{2}{\beta}\right)}\right)} e^{\left(-\frac{\lambda_{\mathrm{R}}(N-1)}{N}\frac{\pi\left(\frac{4\pi}{A_\sigma}\frac{g_s}{G_s}r^4\gamma\right)^{2/\beta}}{\mathrm{sinc}\left(\frac{2}{\beta}\right)}\right)}.\end{aligned} \tag{3}$$

Proof: The proof follows the well-known results in the stochastic geometry literature

$$\begin{aligned}&\mathbb{P}\left[\mathrm{SIR} > \gamma | r, A_\sigma\right]\\ &= \mathbb{P}\left[|h_1|^2 > \frac{4\pi}{A_\sigma}r^4\gamma\sum_{i=2}^{\infty}\frac{G_i}{G_s}\|\mathbf{d}_i - \mathbf{d}_1\|^{-\beta}|h_i|^2\right]\\ &= \mathbb{E}\left[\exp\left(-\frac{4\pi}{A_\sigma}r^4\gamma\sum_{i=2}^{\infty}\frac{G_i}{G_s}\|\mathbf{d}_i - \mathbf{d}_1\|^{-\beta}|h_i|^2\right)\right]\\ &\overset{(a)}{=}\mathbb{E}\left[\prod_{i\in\mathcal{A}}\frac{1}{1+\frac{4\pi}{A_\sigma}r^4\gamma\|\mathbf{d}_i\|^{-\beta}}\right]\cdot\mathbb{E}\left[\prod_{i\in\mathcal{B}}\frac{1}{1+\frac{4\pi}{A_\sigma}\frac{g_s}{G_s}r^4\gamma\|\mathbf{d}_i\|^{-\beta}}\right]\\ &\overset{(b)}{=} e^{\left(-\frac{\lambda_{\mathrm{R}}}{N}\frac{\pi\left(\frac{4\pi}{A_\sigma}r^4\gamma\right)^{2/\beta}}{\mathrm{sinc}\left(\frac{2}{\beta}\right)}\right)} e^{\left(-\frac{\lambda_{\mathrm{R}}(N-1)}{N}\frac{\pi\left(\frac{4\pi}{A_\sigma}\frac{g_s}{G_s}r^4\gamma\right)^{2/\beta}}{\mathrm{sinc}\left(\frac{2}{\beta}\right)}\right)}\end{aligned} \tag{4}$$

where (a) follows Slivnyak's theorem and the Laplace transform of the exponential random variable, and $\mathcal{A}$ is a set of radars that use the same pilot sequence with the tagged radar, while $\mathcal{B}$ is a set of radars a different pilot sequence from the tagged radar. Subsequently, (b) follows the probability generating functional of a PPP. ■

B. Detection Probability

Leveraging Lemma 1, we analyze the detection probability in this section. Theorem 1 is the main result in this section.

Theorem 1: Assuming that ℓ_0, θ_0 are fixed, the detection probability with the threshold γ is

$$\begin{aligned}&P_{\mathrm{detect}}(\gamma)\\ &= \int_0^{\frac{\ell_0\sin(\theta_0-\phi/2)}{2\sin(\phi/2)}} e^{\left(-\frac{\lambda_{\mathrm{R}}}{N}\frac{\pi\left(\frac{4\pi}{\ell_s\sin(\theta_0)}r^4\gamma\right)^{2/\beta}}{\mathrm{sinc}\left(\frac{2}{\beta}\right)}\right)}\\ &\times e^{\left(-\frac{\lambda_{\mathrm{R}}(N-1)}{N}\frac{\pi\left(\frac{4\pi}{\ell_s\sin(\theta_0)}\frac{g_s}{G_s}r^4\gamma\right)^{2/\beta}}{\mathrm{sinc}\left(\frac{2}{\beta}\right)}\right)}\\ &\times e^{-\lambda_{\mathrm{B}}\left(\frac{r\ell_s\sin(\theta_0)}{2}+\lambda_{\mathrm{B}}\frac{L}{\pi}\left|\frac{\ell_s}{2}\cos(\theta_0)-r\right|\right)}2\pi\lambda_{\mathrm{R}}re^{-\lambda_{\mathrm{R}}\pi r^2}\mathrm{d}r\\ &+\int_{\frac{\ell_0\sin(\theta_0-\phi/2)}{2\sin(\phi/2)}}^{\infty} e^{\left(-\frac{\lambda_{\mathrm{R}}}{N}\frac{\pi\left(\frac{4\pi}{\ell_0\sin(\theta_0)}r^4\gamma\right)^{2/\beta}}{\mathrm{sinc}\left(\frac{2}{\beta}\right)}\right)}\\ &\times e^{\left(-\frac{\lambda_{\mathrm{R}}(N-1)}{N}\frac{\pi\left(\frac{4\pi}{\ell_0\sin(\theta_0)}\frac{g_s}{G_s}r^4\gamma\right)^{2/\beta}}{\mathrm{sinc}\left(\frac{2}{\beta}\right)}\right)}\\ &\times e^{-\lambda_{\mathrm{B}}\left(\frac{r\ell_s\sin(\theta_0)}{2}+\lambda_{\mathrm{B}}\frac{L}{\pi}\left|\frac{\ell_s}{2}\cos(\theta_0)-r\right|\right)}2\pi\lambda_{\mathrm{R}}re^{-\lambda_{\mathrm{R}}\pi r^2}\mathrm{d}r\end{aligned} \tag{5}$$

where $\ell_s = 2r\frac{\sin(\phi/2)}{\sin(\theta_0-\phi/2)}$.

Proof: First, we characterize the cross-section area. To do this, we first define the sensing length ℓ_s, which means the maximal blockage length that the tagged radar is able to sense with beamwidth ϕ. Please see Fig. 2 for intuitive description. Using the law of sine, it is easily obtained as $\ell_s = 2r\frac{\sin(\phi/2)}{\sin(\theta_0-\phi/2)}$. As illustrated in Fig. 2, if $\ell_0 < \ell_s$, the cross-section area is defined as $A_\sigma = \ell_0\sin(\theta_0)$ since it is the orthogonal part of the blockage facing the tagged radar. If $\ell_0 > \ell_s$, $A_\sigma = \ell_s\sin(\theta_0)$.

Next we calculate $\mathbb{P}\left[\{E_{\mathrm{block}}\}^c | r\right]$. As shown in Fig. 2, if no blockage exists in the pentagon $T = P + Q + R + S$, the typical blockage is not blocked. We first obtain the area of the corresponding pentagon, denoted as $|T|$, by using the laws of sine and cosine as follows:

$$|T| = \frac{r\ell_s}{2}\sin(\theta_0) + \ell_s'\ell\sin\left(\theta + \theta_0'\right) \tag{6}$$

where $\ell_s' = \sqrt{(\ell_s/2)^2 + r^2 - \ell_s r\cos(\theta_0)}$ and $\theta_0' = \arcsin\left(\frac{\ell_s/2}{\ell_s'}\sin(\theta_0)\right)$. Due to space limitation, we omit the detail proof. With this, we have

$$\begin{aligned}\mathbb{P}\left[\{E_{\mathrm{block}}\}^c\right] &= \prod_{\ell,\theta} e^{(-\lambda_{\mathrm{B}}|T|F_L(\mathrm{d}\ell)F_\Theta(\mathrm{d}\theta))}\\ &= e^{-\lambda_{\mathrm{B}}\frac{r\ell_s\sin(\theta_0)}{2}}e^{-\lambda_{\mathrm{B}}\int_0^\pi\int_0^L\ell_s'\ell\sin\left(\theta+\theta_0'\right)F_L(\mathrm{d}\ell)F_\Theta(\mathrm{d}\theta)}\\ &= e^{-\lambda_{\mathrm{B}}\left(\frac{r\ell_s\sin(\theta_0)}{2}+\frac{L}{\pi}\left|\frac{\ell_s}{2}\cos(\theta_0)-r\right|\right)}.\end{aligned} \tag{7}$$

Incorporating this, we obtain the detection probability conditioned on r as

$$\begin{aligned}&P_{\mathrm{detect}}\left(\gamma \middle| r < \frac{\ell_0\sin(\theta_0-\phi/2)}{2\sin(\phi/2)}\right)\\ &= e^{\left(-\frac{\lambda_{\mathrm{R}}}{N}\frac{\pi\left(\frac{4\pi}{\ell_s\sin(\theta_0)}r^4\gamma\right)^{2/\beta}}{\mathrm{sinc}\left(\frac{2}{\beta}\right)}\right)} e^{\left(-\frac{\lambda_{\mathrm{R}}(N-1)}{N}\frac{\pi\left(\frac{4\pi}{\ell_s\sin(\theta_0)}\frac{g_s}{G_s}r^4\gamma\right)^{2/\beta}}{\mathrm{sinc}\left(\frac{2}{\beta}\right)}\right)}\\ &e^{-\lambda_{\mathrm{B}}\left(\frac{r\ell_s\sin(\theta_0)}{2}+\lambda_{\mathrm{B}}\frac{L}{\pi}\left|\frac{\ell_s}{2}\cos(\theta_0)-r\right|\right)},\end{aligned} \tag{8}$$

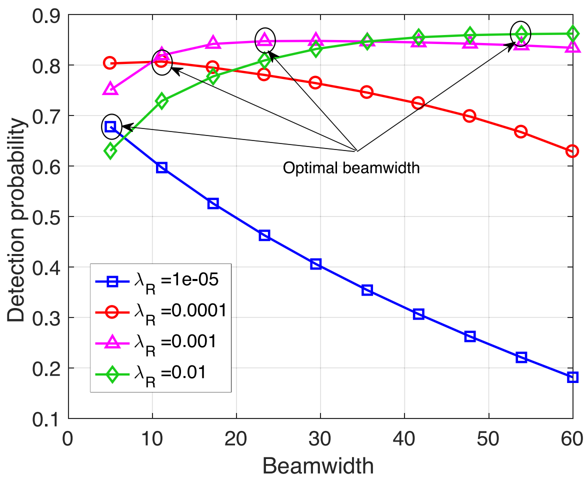

Fig. 3. Detection probability depending on the beamwidth ϕ and the radar density $\lambda_{\rm R}$. The system setting is as follows: $\lambda_{\rm R} \in \{10^{-2}, 10^{-3}, 10^{-4}, 10^{-5}\}$, $\phi \in \{5^\circ, \dots, 60^\circ\}$, $\lambda_{\rm B} = 10^{-4}$, $\beta = 4$, $\ell_0 = 10$, $\theta_0 = 45^\circ$, $\gamma = -20$ dB, $L = 30$, $N = 10$, $G_s = 0$ dB, $g_s = -3$ dB.

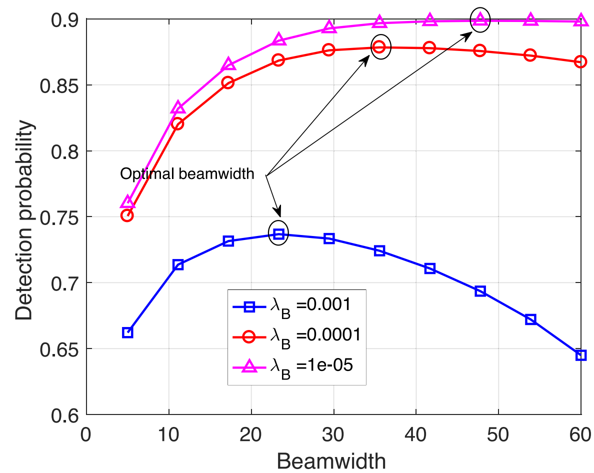

Fig. 4. Detection probability depending on the beamwidth ϕ and the blockage density $\lambda_{\rm B}$. The system setting is as follows: $\lambda_{\rm B} \in \{10^{-3}, 10^{-4}, 10^{-5}\}$, $\phi \in \{5^\circ, \dots, 60^\circ\}$, $\lambda_{\rm R} = 10^{-3}$, $\beta = 4$, $\ell_0 = 20$, $\theta_0 = 45^\circ$, $\gamma = -20$ dB, $L = 30$, $N = 10$, $G_s = 0$ dB, $g_s = -3$ dB.

and

$$P_{\rm detect}\left(\gamma \,\middle|\, r > \frac{\ell_0 \sin(\theta_0 - \phi/2)}{2\sin(\phi/2)}\right) = e^{\left(-\frac{\lambda_{\rm R}}{N}\frac{\pi\left(\frac{4\pi}{\ell_0 \sin(\theta_0)} r^4 \gamma\right)^{2/\beta}}{{\rm sinc}\left(\frac{2}{\beta}\right)}\right)} e^{\left(-\frac{\lambda_{\rm R}(N-1)}{N}\frac{\pi\left(\frac{4\pi}{\ell_0 \sin(\theta_0)}\frac{g_s}{G_s} r^4 \gamma\right)^{2/\beta}}{{\rm sinc}\left(\frac{2}{\beta}\right)}\right)} \times e^{-\lambda_{\rm B}\left(\frac{r\ell_s \sin(\theta_0)}{2} + \lambda_{\rm B}\frac{L}{\pi}\left|\frac{\ell_s}{2}\cos(\theta_0) - r\right|\right)}. \quad (9)$$

Since r follows the well-known first touch distribution of a PPP, incorporating the distribution of r into (8) and (9) completes the proof. ■

We observe that the derived detection probability is a function of system parameters, chiefly the radar and the blockage densities and the radar sensing beamwidth. Using the derived expression, the detection probability is easily evaluated for various system parameters. We note that the detection probability (5) also can be marginalized for ℓ_0 and θ_0 by using the uniform distribution $\mathcal{U}(0, L)$ and $\mathcal{U}(0, \pi)$.

IV. Numerical Results

In this section, we explore how the detection probability varies depending on the system parameters. First, in Fig. 3, we describe the detection probability depending on the beamwidth ϕ and the radar density $\lambda_{\rm R}$ while fixing other system parameters. The system setting is explained in the caption of Fig. 3. Note that there exists an optimal beamwidth $\phi^\star$ that maximizes the detection probability. To understand this, let's assume that ϕ decreases. On the one hand, the cross-section area A_σ decreases and this also decreases the SINR since the reflected signal power is proportional to A_σ. This eventually degrades the detection probability. On the other hand, the probability that other blockages exist in the sensing region decreases, which increases the successful detection probability. The optimal beamwidth balances these two contrary factors so that the maximal detection probability is obtained. Another observation in Fig. 3 is that the optimal beamwidth $\phi^\star$ increases as the radar density $\lambda_{\rm R}$ increases. When $\lambda_{\rm R}$ increases, the distance between the tagged radar and the typical blockage r is likely to decrease. Then the reflected signal power is strong enough so the SINR degradation by decreasing ϕ might be negligible. This means that the performance benefit by increasing ϕ dominates, therefore $\phi^\star$ increases. Finally, it is observed that the detection probability increases as the radar density $\lambda_{\rm R}$ increases, but only with the optimal beamwidth $\phi^\star$. This implies that deploying more radars without using $\phi^\star$ may bring detection performance degradation.

Increasing radar deployment density is cost challenging. One way to minimize the implementation cost is codeploying radars with the communications infrastructure [1]. Another way is for the base station to operate like a radar. For example, in an mmWave communication system, a base station uses directional beamforming while rotating its main-lobe direction to establish initial beam association. A base station can use this to sense the blockages.

In Fig. 4, we depict the detection probability depending on the beamwidth ϕ and the blockage density $\lambda_{\rm B}$. The optimal beamwidth $\phi^\star$ increases as $\lambda_{\rm B}$ decreases. If there are only a few blockages in the network, the probability that other blockages exist in the sensing region is small enough even in the large ϕ. This encourages using large ϕ, resulting in an increase of $\phi^\star$.

V. Conclusion

In this letter, we analyzed the blockage detection probability by using radars in a cellular network. To suitably capture the effects of randomly located radars and blockages, we have exploited a network model based on homogeneous PPPs. Assuming two conditions for successful detection, we have obtained the detection probability as a function of the radar and blockage densities, the beamwidth, and other system parameters. Leveraging the obtained expression, we have had the following three major findings. 1) Deploying more radars is advantageous for detection performance, but only if they use the optimal beamwidth. Without using appropriate beamwidth, deploying more radars might cause performance degradation. 2) The optimal beamwidth increases as more radars are deployed. 3) The optimal beamwidth increases with fewer blockages in the network.

References

[1] N. Gonzalez-Prelcic, R. Mendez-Rial, and R. W. Heath, “Radar aided beam alignment in mmWave V2I communications supporting antenna diversity,” in *Proc. Inf. Theory Appl. Workshop*, Jan. 2016, pp. 1–7.

[2] N. Gonzalez-Prelcic, A. Ali, V. Va, and R. W. Heath, “Millimeter-wave communication with out-of-band information,” *IEEE Commun. Mag.*, vol. 55, no. 12, pp. 140–146, Dec. 2017.

[3] J. Choi, V. Va, N. Gonzalez-Prelcic, R. Daniels, C. R. Bhat, and R. W. Heath, “Millimeter-wave vehicular communication to support massive automotive sensing,” *IEEE Commun. Mag.*, vol. 54, no. 12, pp. 160–167, Dec. 2016.

[4] Y. Li, J. G. Andrews, F. Baccelli, T. D. Novlan, and C. J. Zhang, “Design and analysis of initial access in millimeter wave cellular networks,” *IEEE Trans. Wireless Commun.*, vol. 16, no. 10, pp. 6409–6425, Oct. 2017.

[5] J. Rodriguez-Fernndez, N. Gonzalez-Prelcic, K. Venugopal, and R. W. Heath, “Frequency-domain compressive channel estimation for frequency-selective hybrid millimeter wave MIMO systems,” *IEEE Trans. Wireless Commun.*, vol. 17, no. 5, pp. 2946–2960, May 2018.

[6] S. S. Raymond, A. Abubakari, and H. S. Jo, “Coexistence of power-controlled cellular networks with rotating radar,” *IEEE J. Sel. Areas Commun.*, vol. 34, no. 10, pp. 2605–2616, Oct. 2016.

[7] B. Li, A. P. Petropulu, and W. Trappe, “Optimum co-design for spectrum sharing between matrix completion based MIMO radars and a MIMO communication system,” *IEEE Trans. Signal Process.*, vol. 64, no. 17, pp. 4562–4575, Sep. 2016.

[8] A. Al-Hourani, R. J. Evans, S. Kandeepan, B. Moran, and H. Eltom, “Stochastic geometry methods for modeling automotive radar interference,” *IEEE Trans. Intell. Transp. Syst.*, vol. 19, no. 2, pp. 333–344, Feb. 2018.

[9] T. Bai, R. Vaze, and R. W. Heath, “Using random shape theory to model blockage in random cellular networks,” in *Proc. Int. Conf. Signal Process. Commun.*, Jul. 2012, pp. 1–5.